Harmful Algae 115 (2022) 102191

Contents lists available at ScienceDirect

Harmful Algae

journal homepage: www.elsevier.com/locate/hal

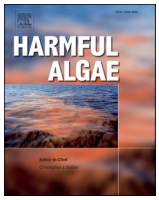

# A validation of satellite derived cyanobacteria detections with state reported events and recreation advisories across U.S. lakes

Peter Whitman [a,*], Blake Schaeffer [b], Wilson Salls [b], Megan Coffer [a,c], Sachidananda Mishra [d,e], Bridget Seegers [f,g], Keith Loftin [h], Richard Stumpf [e], P. Jeremy Werdell [f]

[a] Oak Ridge Institute for Science and Education, U.S. Environmental Protection Agency, Durham, NC 27709, USA
[b] U.S. Environmental Protection Agency, Office of Research and Development, Durham, NC 27709, USA
[c] Center for Geospatial Analytics, North Carolina State University, Raleigh, NC 27606, USA
[d] Consolidated Safety Services Inc. Fairfax, VA 22030, USA
[e] National Oceanic and Atmospheric Administration, National Centers for Coastal Ocean Science, Silver Spring, MD, USA
[f] Ocean Ecology Laboratory, NASA Goddard Space Flight Center, Greenbelt, MD, USA
[g] Universities Space Research Association, Columbia, MD, USA
[h] U.S. Geological Survey, Kansas Water Science Center, Lawrence, KS, USA

ARTICLE INFO

[AW]

*Keywords:*
Satellite
Water quality
Cyanobacteria
Human health
Recreation advisory
Validation

ABSTRACT

Cyanobacteria harmful algal blooms (cyanoHABs) negatively affect ecological, human, and animal health. Traditional methods of validating satellite algorithms with data from water samples are often inhibited by the expense of quantifying cyanobacteria indicators in the field and the lack of public data. However, state recreation advisories and other recorded events of cyanoHAB occurrence reported by local authorities can serve as an independent and publicly available dataset for validation. State recreation advisories were defined as a period delimited by a start and end date where a warning was issued due to detections of cyanoHABs over a state's risk threshold. State reported events were defined as any event that was documented with a single date related to cyanoHABs. This study examined the presence-absence agreement between 160 state reported cyanoHAB advisories and 1,343 events and cyanobacteria biomass estimated by a satellite algorithm called the Cyanobacteria Index ($CI_{cyano}$). The true positive rate of agreement with state recreation advisories was 69% and 60% with state reported events. $CI_{cyano}$ detected a reduction or absence in cyanobacteria after 76% of the recreation advisories ended. $CI_{cyano}$ was used to quantify the magnitude, spatial extent, and temporal frequency of cyanoHABs; each of these three metrics were greater ($r > 0.2$) during state recreation advisories compared to non-advisory times with effect sizes ranging from small to large. This is the first study to quantitatively evaluate satellite algorithm performance for detecting cyanoHABs with state reported events and advisories and supports informed management decisions with satellite technologies that complement traditional field observations.

## 1. Introduction

Cyanobacteria are photosynthetic bacteria found in freshwater ecosystems worldwide. Elevated levels of nutrients and warm temperatures are often associated with cyanobacterial harmful algal blooms (cyanoHABs) (Merel et al., 2013; Paerl, 2008; Paerl et al., 2011). CyanoHABs may produce cyanotoxins that can negatively affect human and animal health by causing neurological damage, liver damage, skin irritation, and respiratory problems (Backer et al., 2010; Backer et al., 2013; Backer et al., 2015; Carmichael and Boyer, 2016). Even when cyanotoxins are absent, cyanoHABs may adversely affect commercial fisheries (Dodds et al., 2009) and ecological health by creating hypoxic conditions. Additionally, cyanoHABs have a negative aesthetic perception that can affect tourism and property values (Wolf et al., 2017), which is exacerbated by their tendency to concentrate around shorelines (Chorus et al., 2000). The full scope of pecuniary consequences related to cyanoHABs is illustrated by Stroming et al., (2020), who found that the approximate socioeconomic costs of a single cyanoHAB event in Utah Lake, Utah were valued at $370,000.

Comprehensive monitoring of cyanoHABs across lakes used for recreation or drinking water may minimize economic losses and reduce human and animal health effects (Stroming et al., 2020). The U.S.

* Corresponding author.
*E-mail address:* whitman.peter@epa.gov (P. Whitman).

https://doi.org/10.1016/j.hal.2022.102191
Received 1 October 2021; Received in revised form 7 January 2022; Accepted 26 January 2022
Available online 12 May 2022

Environmental Protection Agency (EPA) has published health advisory recommendations for cyanotoxin exposure levels in lakes used for recreation and drinking water (U.S. Environmental Protection Agency, 2019a, 2019b) and the World Health Organization provides a monitoring and management framework based on cyanobacteria and cyanotoxin thresholds (Chorus and Welker, 2021; World Health Organization, 2003). However, exposure risk thresholds based on cell counts, toxin concentrations, or other measures have not been uniformly adopted by state monitoring programs in the United States (Graham et al., 2009; Ibelings et al., 2015; Stone and Bress, 2007). This can be partially attributed to the expense associated with quantifying cyanobacteria cell counts and cyanotoxin concentrations (Merel et al., 2013), which motivates states to use a variety of alternative measures to assess cyanoHAB exposure risk (Interstate Technology & Regulatory Council, 2021). These measures may include visual assessments (U.S. Environmental Protection Agency, 2019b), jar and stick tests (Austin et al., 2018), satellite remote sensing (Wyoming Department of Environmental Quality, 2018), genetic methods (Ohio Environmental Protection Agency, 2019), fluorometric detection of pigments (New York Department of Environmental Conservation, 2020), automated classification systems (Deglint et al., 2018), or any combination of these methods. The spatial and temporal coverage of *in situ* methods can be limited due to the time, labor, and cost required to routinely monitor a large number of lakes in the field (Papenfus et al., 2020). Satellite remote sensing has been shown to complement *in situ* methods by providing broader spatial and temporal detection of cyanoHABs that can be standardized throughout the United States (Schaeffer et al., 2015).

There has been extensive development of satellite ocean color remote sensing methods to detect cyanoHABs in inland lakes (Binding et al., 2012; Hu et al., 2010; Matthews and Odermatt, 2015; Mishra et al., 2013; Shi et al., 2017; Simis et al., 2005; Stumpf et al., 2012; Wynne et al., 2010). While satellite observations cannot directly detect cyanotoxins because they do not produce an optical signature (Stumpf et al., 2016), these studies have shown that satellite sensors can be used to detect and quantify proxies of cyanobacteria biomass within lakes and estuaries (Kutser, 2009). Here we focus on the Cyanobacteria Index ($CI_{cyano}$), which relies on two spectral shape algorithms in concert to provide per-pixel estimates of cyanobacteria biomass within images collected by the European Space Agency's MEdium Resolution Imaging Spectrometer (MERIS) and Ocean and Land Colour Instrument (OLCI).

$CI_{cyano}$ was originally developed using data collected in western Lake Erie (Wynne et al., 2008) and was later updated and assessed in Ohio, Florida, and eight northeastern U.S. states (Clark et al., 2017; Lunetta et al., 2015). Three summary indicator metrics have subsequently been developed to characterize the cyanobacteria biomass detected by $CI_{cyano}$ within lakes and waterbodies. They include magnitude (Mishra et al., 2019), spatial extent (Urquhart et al., 2017), and temporal frequency (Clark et al., 2017; Coffer et al., 2021a). Magnitude is the spatiotemporal mean of weekly maximum $CI_{cyano}$ values for a defined observation period (Mishra et al., 2019). Spatial extent is the area of unique pixels where cyanobacteria have been detected with $CI_{cyano}$ within a defined observation period (Urquhart et al., 2017). Temporal frequency is the spatially averaged fraction of total satellite observations where cyanobacteria have been detected with $CI_{cyano}$ within a defined observation period (Clark et al., 2017; Coffer et al., 2021a). Temporal frequency and magnitude have been used together to evaluate the characteristics of cyanobacteria biomass at drinking water intakes (Coffer et al., 2021b).

While it is traditional to validate satellite algorithms with quantitative measurements of cyanobacteria, such as pigment concentrations, biomass, or other common biogeophysical measures, sometimes this is not possible. In these cases, alternative proxy sources of information can be considered, such as newspaper articles, state advisories, and other recorded events that follow the direct identification or quantification of cyanoHAB presence by local authorities (Yagoub et al., 2020). State recreation advisories and state reported events provide independent, common, and publicly accessible records of cyanoHABs. Here, state recreation advisories are defined as a distinct period delimited by a start and end date where a caution, warning, or closure is issued due to detections of cyanoHABs over a state's risk threshold for cyanobacteria cell counts or cyanotoxin concentrations. State reported events are more loosely defined as any event related to cyanoHABs that was documented with a single date, which could include responses to citizen reports, sampling, following up on received complaints that may or may not be cyanoHAB related, or a state action reported to the Natural Resources Defense Council (NRDC). Despite some limitations due to erroneous reports and limited geolocation information, state documentation of events and recreation advisories are considered a reliable source. Yet there are only a limited number of studies, such as Mishra et al., (2021), that focus on comparisons between independent state reports of cyanoHABs and satellite-derived estimates. As such, additional validation of satellite algorithms against independent state reports of cyanoHABs may support the implementation and performance assessment of satellite remote sensing technology into future comprehensive cyanoHAB monitoring plans.

This study examined the presence and absence agreement between recreation advisories and state reported cyanoHAB events with satellite remote sensing detection of cyanobacteria biomass derived from the MERIS and OLCI sensors. In particular, this study addressed the following questions: (1) Does the Cyanobacteria Index ($CI_{cyano}$) detect cyanobacteria presence during state cyanoHAB events and recreation advisories? (2) Does $CI_{cyano}$ detect a reduction in cyanobacteria after the recreation advisory end date? (3) Are there differences between temporal frequency, spatial extent, or magnitude quantified using $CI_{cyano}$ during state recreation advisories compared to non-advisory times?

## 2. Data and methods

### 2.1. State reported events

A publicly available dataset of cyanoHAB state reported events that occurred in the conterminous United States (CONUS) between 2008 to 2018 was downloaded from the Natural Resources Defense Council (NRDC) at https://www.nrdc.org/harmful-algal-blooms-methodology. The NRDC compiled the dataset by soliciting data from state agencies (Natural Resource Defence Council, 2019). Because many states use different thresholds and sampling methods, these events include any type of response that may be related to a harmful algal bloom (HAB) including a cyanotoxin detection, reported illness, issued advisory, reported cyanoHAB or other HAB, or exceeded threshold. Data attributes for each record included the state, date of the event, latitude/longitude coordinates when available, lake name, and method of detection. It is important to note that there was no record of the specific *in situ* sampling method or analysis for any of the records, only a general observation category related to either cyanobacteria, cyanotoxins, or reported illness. Furthermore, event-based sampling is usually conducted from shore where cyanobacteria biomass can accumulate while nearshore satellite retrievals are typically discarded because they can be adulterated by bottom reflectance and land surface reflectance.

### 2.2. State recreation advisories

State recreation advisories that occurred across CONUS between 2008 and 2019 were identified from the U.S. EPA's monthly cyanoHAB newsletter records of "Blooms, beach closures and health advisories" (https://www.epa.gov/cyanohabs/epa-newsletter-and-collaboration-and-outreach-habs#news). These newsletters contain a monthly summary of all known cautions, warnings, advisories, or closures due to the presence of cyanobacteria, cyanotoxins, or both. In addition, the newsletters provide links to each state's cyanoHAB website where dates delimiting the start and end date of each advisory could be accessed (Table S1). Data collection from these state websites was limited to publicly accessible information. Compared to the dataset of state

reported events, the two distinguishing characteristics of the state recreation advisory dataset were as follows: (1) each record included the start and end date of the advisory period, and (2) each advisory was initiated using measurements of cyanobacteria cell counts and/or cyanotoxin concentrations as opposed to visual indicators or other observations, although the thresholds used by each state were not consistent and could change over time. Common attributes provided for each record included the name of the lake where the state recreation advisory was issued, the state in which that lake was located, and the dates that the advisory started and ended.

Although limited programs may provide routine sampling as resources permit, state cyanoHAB monitoring typically occurs opportunistically or in response to reported cyanoHABs (Backer et al., 2015). Therefore, sampling was likely overweighted toward cyanoHAB presence and underweighted during times of minimal or no cyanoHABs. Sampling was also seasonally biased toward the recreation season, typically from Memorial Day (end of May) to Labor Day (beginning of September), but this can vary with some states that report advisories well into the late fall (e.g. Pacific Northwest) or throughout the winter (e.g. Southeast and South Central United States). The seasonal bias was similar to that previously reported from the data available in the U.S. Water Quality Portal (Papenfus et al., 2020; Schaeffer et al., 2018a). Thresholds and decision criteria to end recreation advisories vary across states and develop over time. Therefore, no single baseline could be assumed as a common action threshold. A brief summary of the current thresholds for the nine states with recreation advisories included in this study highlight the dynamic range of potential responses (Table S2). These variations in sampling frequency, thresholds, and procedure could be a potential source of mismatch with satellite observations.

### 2.3. $CI_{cyano}$ daily product

Cyanobacteria data products derived from MERIS and OLCI were obtained from the National Aeronautics and Space Administration (NASA) Ocean Color website (https://oceancolor.gsfc.nasa.gov/projects/cyan/). Both MERIS and OLCI are satellite sensors that provide an archive of imagery with 300-m spatial resolution at approximately two- to three-day intervals over CONUS. The MERIS archive contains imagery captured from 2002 to 2012 and the ongoing OLCI archive began in 2016. The four-year gap between the two sensors exists because the Envisat mission, which housed MERIS, ended in April 2012 and Sentinel-3A, which houses the first OLCI sensor, did not become available until February 2016. The addition of a second OLCI sensor after the launch of Sentinel-3B in April 2018 resulted in near-daily imagery collected by OLCI sensors in concert across CONUS. MERIS coverage was less reliable over CONUS prior to 2008, so the cyanobacteria data products used in this study were limited to January 2008 through April 2012 and February 2016 through July 2019.

The cyanobacteria data products were produced using $CI_{cyano}$, which is an index that relies on two spectral shape algorithms in tandem to produce per-pixel estimates of cyanobacteria biomass. It is an update to the Cyanobacteria Index (CI) developed by Wynne et al., (2008), which incorporates improvements defined by Matthews et al., (2012, Eqs. 3 and 4) that separate cyanobacteria from other algal biomass (Lunetta et al., 2015). $CI_{cyano}$ algorithm performance has been previously validated quantitatively (Clark et al., 2017; Coffer et al., 2021b; Lunetta et al., 2015; Mishra et al., 2021) and qualitatively (Schaeffer et al., 2018b). The complete sequence of $CI_{cyano}$ development is described in greater detail in Coffer et al., (2020) and briefly reviewed here.

Level-1B MERIS and OLCI data are processed to Level-2 data by the NASA Ocean Biology Processing Group (OBPG) using the satellite processing module l2gen. The output of l2gen is Rayleigh-corrected reflectance, which is thresholded to mask image pixels containing clouds and sun glint (Wynne et al., 2018). Land is masked from each image using NASA Shuttle Radar Topography Mission Water Body Data in conjunction with a thresholding approach that identifies mixed land-water pixels (Wynne et al., 2018). After the masks are applied, $CI_{cyano}$ is calculated from spectral shape algorithms using the following equation (Matthews et al., 2012; Wynne et al., 2008):

$$SS(\lambda) = \rho_s(\lambda) - \rho_s(\lambda^-) - \{\rho_s(\lambda^+) - \rho_s(\lambda^-)\} * \frac{(\lambda - \lambda^-)}{(\lambda^+ - \lambda^-)} \quad (1)$$

where $SS$ is the spectral shape, $\rho_s$ is Rayleigh-corrected reflectance, $\lambda$ is the central spectral band of interest, and $\lambda_+$ and $\lambda_-$ are the adjacent reference spectral bands above and below the central spectral band, respectively. Wynne et al., (2008) used this equation to assess cyanobacteria presence within MERIS imagery with $\lambda$ as 681 nanometers (nm), $\lambda^+$as 709 nm, and $\lambda^-$ as 665 nm. These authors discovered that when $SS(681)$ was below zero (i.e., the spectral shape was concave) cyanobacteria were present, and when $SS(681)$ was above zero (i.e., convex), there were no cyanobacteria present. It was postulated that this phenomenon could be attributed to cyanobacteria having a much lower fluorescence signal at 681 nm than eukaryotic phytoplankton. The original CI was computed from this $SS$ and can be represented using the following notation:

$$CI = \begin{cases} |SS(681)| & if\ SS(681) < 0 \\ 0 & otherwise \end{cases} \quad (2)$$

Lunetta et al., (2015) incorporated a second $SS$ calculation proposed by Matthews et al., (2012) that provides an additional exclusion criterion, with $\lambda$ as 665 nm, $\lambda^+$as 681 nm, and $\lambda^-$ as 620 nm. This second $SS$ algorithm centers around 665 nm because the elevated presence of the phycocyanin pigment associated with cyanobacteria depresses reflectance at 620 nm, which causes $SS(665)$ to be greater than zero. $CI_{cyano}$ can be defined using the following notation:

$$CI_{cyano} = \begin{cases} CI & if\ SS(665) > 0 \\ 0 & otherwise \end{cases} \quad (3)$$

Therefore, pixel values derived from $CI_{cyano}$ that are greater than zero represent a detection of cyanobacteria abundance and values of zero represent a valid observation of a lake surface with no detection of cyanobacteria. In addition to the pixels providing estimates of cyanobacteria abundance, the $CI_{cyano}$ product also contains the pixels that were masked because they contain observations of land or for quality assurance (QA) because they provide an observation of clouds or sun glint on the water surface (Wynne et al., 2018). An example of the $CI_{cyano}$ product is demonstrated in Fig. 1 and a conceptual representation of the methods described in Sections 2.3 through 2.5 is provided in Fig. 2.

### 2.4. $CI_{cyano}$ bloom presence and absence

For each satellite pixel, $CI_{cyano}$ products were composited into seven-day rolling maximums across the entire time period of observations for both MERIS (2008 through 2012) and OLCI (2016 through 2019). In so doing, the first seven-day maximum composite using MERIS imagery included images collected from 1 January 2008 through 7 January 2008 and for each satellite pixel, the maximum $CI_{cyano}$ data value measured during this time period was preserved; a date of 1 January 2008 was assigned to this composite. The second seven-day maximum composite summarized imagery collected from 2 January 2008 through 8 January 2008, the third summarized 3 January 2008 through 9 January 2008, and so forth. The date assigned to each seven-day maximum composite was used to match composites to the dates provided with each record of state reported events and recreation advisories.

The seven-day maximum compositing approach was used to account for day-to-day fluctuations in surficial cyanobacteria presence that occurs due to a combination of water column mixing cycles and buoyancy control mechanisms (Wynne and Stumpf, 2015). It was also used to minimize gaps in the satellite data that result from limited satellite overpasses and days without data because of cloudy conditions. Similar

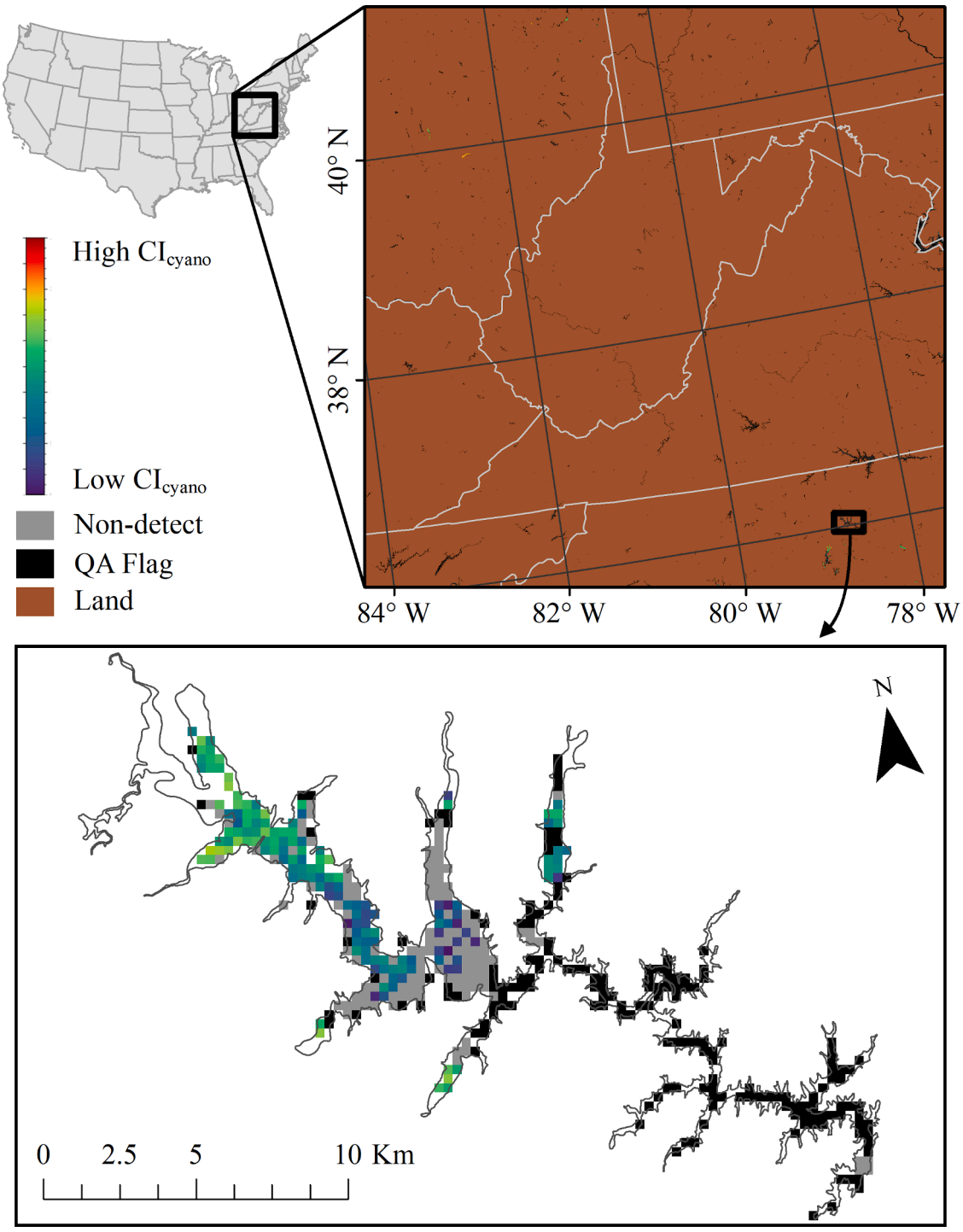


**Fig. 1.** A seven-day maximum composite of $CI_{cyano}$ output derived from satellite imagery captured between July 5 and July 11, 2020. The brown pixels are land and black pixels are flagged by QA masks. The colored pixels represent $CI_{cyano}$ estimates of cyanobacteria from low (purple) to high (red). Gray pixels are a valid observation of the lake surface with no detection of cyanobacteria. Land pixels were removed from the close-up of Falls Lake, North Carolina at the bottom of the Fig. to highlight the pixels that correspond to the resolvable lake surface. These were the pixels used to establish $CI_{cyano}$ bloom presence and absence in this study.

compositing approaches have been used extensively with $CI_{cyano}$ data in the past (Clark et al., 2017; Coffer et al., 2020; Coffer et al., 2021a; Coffer et al., 2021b; Lunetta et al., 2015; Mishra et al., 2019; Urquhart et al., 2017). Lunetta et al., (2015) noted that there was very little variability in the results of their $CI_{cyano}$ validation when using temporal windows ranging from 3 to 15 days in duration. There was no further analysis conducted to examine the impact that compositing and the length of the compositing window might have on the results of this study.

Each lake was evaluated to determine if a cyanoHAB was present based on cyanobacteria magnitude and spatial extent, which were computed from each seven-day $CI_{cyano}$ maximum composite (Fig. 2). There were three possible outcomes of this evaluation: (1) $CI_{cyano}$ bloom presence, (2) $CI_{cyano}$ bloom absence, or (3) insufficient data for evaluation. $CI_{cyano}$ bloom presence occurred if $CI_{cyano}$ magnitude, computed as the mean of the $CI_{cyano}$ values within the seven-day composite, was greater than or equal to the algorithm detection limit of 0.0001 and the spatial extent, computed as the area of unique pixels where

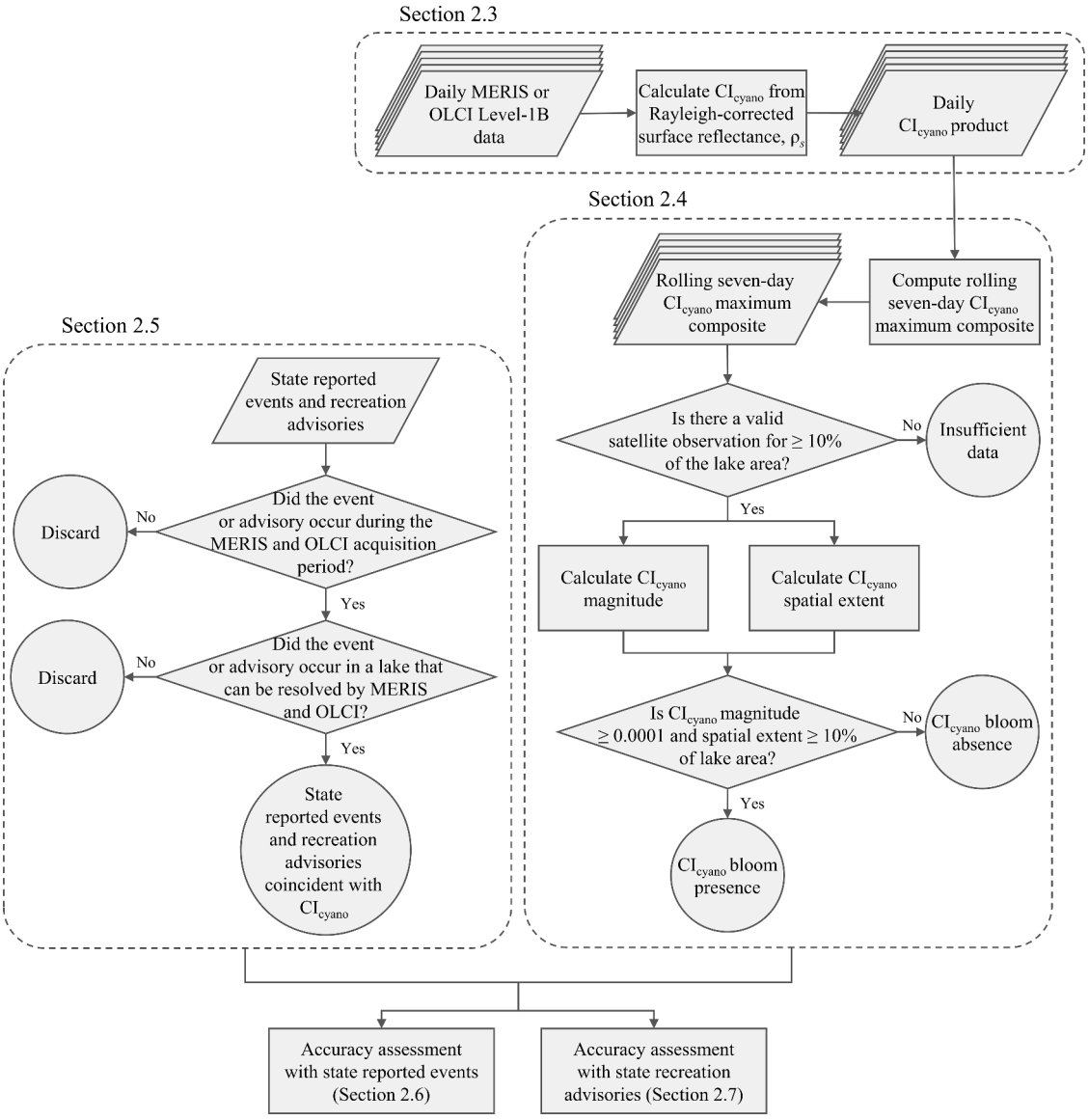


**Fig. 2.** A representation of the approach used to examine agreement between state reported events and state recreation advisories and $CI_{cyano}$ bloom presence and absence.

cyanobacteria have been detected with $CI_{cyano}$ within the seven-day composite, was greater than or equal to 10% of the lake area. $CI_{cyano}$ bloom absence occurred when there was sufficient data for evaluation but the aforementioned criteria for bloom presence were not met. Insufficient data for evaluation occurred if greater than 90% of the pixels that made up that lake had been flagged by the QA mask. The 10% spatial extent threshold was previously tested by Coffer et al., (2020) who discovered that spatial thresholds less than 10% can over classify cyanoHAB presence and spatial thresholds greater than 10% can under classify cyanoHAB presence, particularly in larger lakes and reservoirs. In addition, while a different compositing approach could be chosen that does not involve the maximum $CI_{cyano}$ value, it would have little impact on the results of this study because the magnitude criterion is designed so that any detection of cyanobacteria in greater than or equal to 10% of a lake is considered a $CI_{cyano}$ bloom presence. This criteria was based on guidance from the World Health Organization that recommends conservative overestimates of cyanobacteria as a precautionary measure to ensure human and animal health when cyanotoxin data is not available (Ibelings et al., 2021).

### *2.5. State reported events and recreation advisories coincident with $CI_{cyano}$*

State reported events and state recreation advisories were considered for any lake that was resolvable by the MERIS and OLCI satellite sensors across CONUS during 2008-2012 and 2016-2019 (Fig. 2). The spatial resolution of MERIS and OLCI is 300-m and only lakes of sufficient size and shape to accommodate at least three, 300-m satellite pixels were considered for this analysis. Lakes that are resolvable by these satellites were identified according to Clark et al., (2017). A total of 2,321 lakes across CONUS were classified as resolvable with at least one lake in each state, except for West Virginia and Delaware. Therefore, it is important to note that because many smaller waterbodies cannot be resolved by the MERIS and OLCI sensors and many waterbodies have never been monitored or are not routinely monitored by states, these datasets of state reported events and recreation advisories do not represent a complete list of all cyanoHABs that occurred in the United States during the time period of this study.

### 2.6. Agreement assessment with state reported events

Each state reported event record included the date that the observation of a cyanoHAB occurred. This single date was used to select the appropriate $CI_{cyano}$ composite to determine if there was a co-occurring $CI_{cyano}$ bloom presence in the lake where the event arose. This assessment had two outcomes: (1) presence-presence and (2) misfit absence because the state reported events records provided no observations of cyanoHAB absence, which prevented an assessment of the misfit presence and absence-absence scenarios that are described in the next section. If there was $CI_{cyano}$ bloom presence for the seven-day maximum composite corresponding to the date of the state reported event, the result was recorded as presence-presence. Conversely, if there was a $CI_{cyano}$ bloom absence, the result was recorded as misfit absence. Field and satellite monitoring both include unquantifiable error and do not represent truth; therefore when there was a discrepancy between the two results it was labelled misfit to avoid the presumption that either was truth (Lynch et al., 2009). The presence-presence and misfit absence scenarios correspond to the top-left and bottom-left positions, respectively, in the confusion matrix presented in Fig. 3.

### 2.7. Agreement assessment with state recreation advisories

Each state recreation advisory was delimited by a start and end date that indicated when a lake exceeded a state's cyanoHAB thresholds and when that lake dropped below the state's thresholds. These dates were used to select the appropriate $CI_{cyano}$ composites for each advisory to determine if a $CI_{cyano}$ bloom presence occurred. There were two outcomes of this assessment: (1) presence-presence and (2) misfit absence. If there was a $CI_{cyano}$ bloom presence at any time during a state recreation advisory, the result was recorded as presence-presence. If there were only $CI_{cyano}$ bloom absences observed during the advisory period, the result was recorded as misfit absence. As with the state reported events, the presence-presence and misfit absence scenarios correspond to the top-left and bottom-left positions, respectively, in the confusion matrix presented in Fig. 3.

The dataset of state recreation advisories did not include records of true cyanoHAB absence because it would require routine monitoring that is time consuming and costly to implement using traditional field-based methods. However, each state recreation advisory did include the date that the advisory ended, which was used as a pseudo-absence to denote when a reduction in $CI_{cyano}$ should be expected. There were two outcomes of this assessment: (1) absence-absence and (2) misfit presence. If there was a $CI_{cyano}$ bloom absence in the seven-day composite after the advisory ended, or $CI_{cyano}$ was substantively lower in the week after an advisory ended compared to the advisory time period, the result was recorded as an absence-absence. The substantive difference in $CI_{cyano}$ between the week after an advisory ended compared to the advisory time period was quantified using a nonparametric two-sample test for independent data called the Mann-Whitney *U*. This test provides the ability to examine the alternative hypothesis that a sample of $CI_{cyano}$ data taken during the advisory period is substantively greater than a sample of $CI_{cyano}$ data taken from the week after the advisory period ended (Mann and Whitney, 1947). It is effectively a count of the times that a score from one sample precedes a score from another sample in rank order (Mann and Whitney, 1947). The results of the test were further distilled into an effect size following the Wendt (1972) formulation of rank biserial correlation:

$$r = 1 - \frac{2U}{n_1 * n_2} \tag{4}$$

where $U$ is the Mann-Whitney test statistic, $n_1$ is the number of observations during the advisory period, and $n_2$ is the number of observations in the week after the advisory period ended. The effect size $r$ was classified according to the scheme introduced by Cohen (1988) for correlation coefficients so that values between 0.1 and 0.3 indicate a small difference between samples, values between 0.3 and 0.5 indicate a moderate difference between samples, and values above 0.5 indicate a large difference between samples. $CI_{cyano}$ was considered substantively lower in the week after an advisory ended and recorded as an absence-absence when $r$ was greater than 0.3. Conversely, if there was a $CI_{cyano}$ bloom presence in the seven-day composite after the advisory ended, or $CI_{cyano}$ was not substantively lower ($r < 0.3$) in the week after an advisory ended compared to the advisory time period, the result was recorded as a misfit presence. While not ideal, a strict threshold for $r$ was required to be able to group results, so a cutoff was selected based on the lower bound of a moderate effect. The absence-absence and misfit presence scenarios correspond to the bottom-right and top-right positions, respectively, in the confusion matrix presented in Fig. 3.

### 2.8. $CI_{cyano}$ performance metrics

$CI_{cyano}$ performance was quantified with a suite of metrics that synthesize the agreement measures computed in Section 2.6 and Section 2.7. While all metrics were used to quantify the performance of $CI_{cyano}$ when it was compared to state recreation advisories, the state reported event records did not permit the use of metrics that required absence-absence or misfit absence. *Overall agreement* is the sum of correctly classified counts over the total sample count; it summarizes $CI_{cyano}$ performance under the assumption that the presence and absence categories have similar sample counts, which is the case with this study (Eq. 5). Assessment of $CI_{cyano}$ performance was additionally calculated for presence and absence classes separately to account for unbalanced sample counts. The *true positive rate* gives the proportion of state

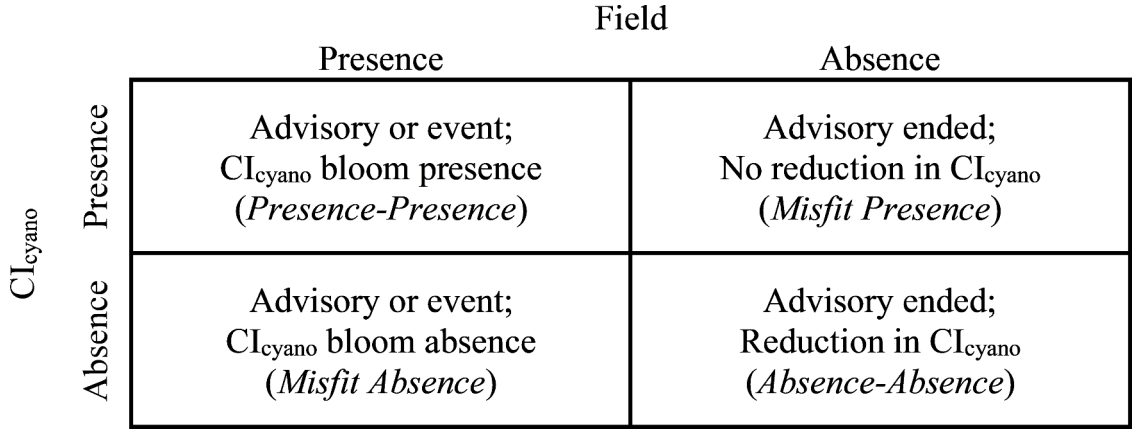


**Fig. 3.** A conceptual confusion matrix that outlines the four scenarios used to evaluate agreement between field monitoring and $CI_{cyano}$ bloom presence and absence.

reported events or state recreation advisories where a $CI_{cyano}$ bloom presence was observed (Eq. 6). The *true negative rate* gives the proportion of state recreation advisories where an advisory was lifted and a reduction in $CI_{cyano}$ or a $CI_{cyano}$ bloom absence was observed (Eq. 7). The *positive predictive value* provides the probability that a $CI_{cyano}$ bloom presence will coincide with the presence of what would be considered a cyanoHAB in the field (Eq. 8). *Negative predictive value* provides the probability that a reduction in $CI_{cyano}$ or a $CI_{cyano}$ bloom absence coincides with what would be considered a cyanoHAB absence or reduction in the field (Eq. 9). The *F1 score* can be interpreted as a weighted average of the positive predictive value and true positive rate, where an F1 score reaches its best value at 1 and worst value at 0 (Eq. 10). The relative contribution of the positive predictive value and true positive rate are equal which makes the F1 score insensitive to unbalanced sample counts.

$$Overall\ Agreement = \frac{Presence - Presence + Absence - Absence}{Total} \quad (5)$$

$$True\ Positive\ Rate\ (TPR) = \frac{Presence - Presence}{Presence - Presence + Misfit\ Absence} \quad (6)$$

$$True\ Negative\ Rate\ (TNR) = \frac{Absence - Absence}{Absence - Absence + Misfit\ Presence} \quad (7)$$

$$Positive\ Predictive\ Value\ (PPV) = \frac{Presence - Presence}{Presence - Presence + Misfit\ Presence} \quad (8)$$

$$Negative\ Predictive\ Value\ (NPV) = \frac{Absence - Absence}{Absence - Absence + Misfit\ Absence} \quad (9)$$

$$F1\ Score = 2 * \frac{PPV * TPR}{PPV + TPR} \quad (10)$$

### 2.9. Sensitivity of $CI_{cyano}$ indicator metrics to state recreation advisories

Three indicator metrics, magnitude (Mishra et al., 2019), spatial extent (Urquhart et al., 2017), and temporal frequency (Clark et al., 2017; Coffer et al., 2021a), were used to determine if cyanobacteria biomass was detected by $CI_{cyano}$ more frequently, across greater spatial extent, or with increased magnitude during state recreation advisory periods compared to periods without state recreation advisories. For each lake, magnitude was calculated as the spatiotemporal mean of seven-day maximum $CI_{cyano}$ values for a defined observation period (Mishra et al., 2019). Spatial extent was computed as the median number of unique pixels where cyanobacteria was detected with $CI_{cyano}$ within a defined observation period (Urquhart et al., 2017). Temporal frequency was calculated as the fraction of seven-day maximum composites where a $CI_{cyano}$ bloom presence occurred during a defined observation period (Clark et al., 2017; Coffer et al., 2021a). The defined observation periods used to calculate frequency, magnitude, and extent were delimited by the state recreation advisories. For each lake with one or more advisories, each indicator metric was calculated using $CI_{cyano}$ data from outside of all advisory dates and then again using $CI_{cyano}$ data from within all advisory dates. This produced a set of paired dependent samples for each metric. Two study timeframes were included in the analysis: (1) the entire MERIS and OLCI time periods and (2) the recreation season between May 1$^{st}$ and October 31$^{st}$ for all years in the MERIS and OLCI time series to examine the effects of seasonality.

The substantive difference in $CI_{cyano}$ metrics between periods with a state recreation advisory and periods without a state recreation advisory was quantified using a nonparametric two-sample test for dependent data called the Wilcoxon signed-rank test (Wilcoxon, 1945). This test provides the ability to evaluate the alternative hypothesis that a $CI_{cyano}$ metric derived from data within an advisory period is substantively greater than a $CI_{cyano}$ metric derived from data outside of an advisory period. When the number of paired observations $n$ is greater than or equal to 20, as is the case in this study, the distribution of the Wilcoxon signed-rank test statistic $W$ converges to a normal distribution and a z-score can be calculated following Siegel (1956). A $CI_{cyano}$ metric was considered greater during advisory periods than outside of advisory periods if it had a large, positive $z$-score and a small $p$-value. An effect size $r$ was also calculated for each metric by dividing the $z$-score by the square root of $n$ (Fritz et al., 2012). The effect size $r$ was classified according to the scheme introduced by Cohen (1988) for correlation coefficients so that values between 0.1 and 0.3 indicate a small difference between samples, values between 0.3 and 0.5 indicate a moderate difference between samples, and values above 0.5 indicates a large difference between samples.

## 3. Results and Discussion

### 3.1. State reported events

There were 1,343 events retained after the state reported events were filtered to match coincident MERIS and OLCI imagery. The 1,343 events occurred in 210 lakes across 26 states (Fig. 4). In descending order, the five states with the greatest number of state reported events were Iowa (601), Vermont (139), North Carolina (101), Ohio (67), and California (59). Of the 1,343 cyanoHAB events, 1,247 occurred between May and October, which indicated a strong seasonal pattern in sampling frequency that is likely caused by seasonal increases in cyanoHAB occurrence and corresponding sampling bias. CyanoHABs observed by $CI_{cyano}$ in the 210 lakes with state reported events reached a maximum in the late summer and fall of each year for both MERIS and OLCI (Fig. 5). This pattern coincides with previously reported nationwide cyanoHAB occurrence phenology for the United States (Graham et al., 2017; Luglie et al., 2017; Xu et al., 2016). Furthermore, the subset of lakes with state reported events presented cyanoHAB occurrence phenology that was similar to the 2,321 lakes that can be resolved by MERIS and OLCI (Coffer et al., 2020) and displayed no unique patterns that might indicate these lakes experienced different cyanobacteria dynamics. Based on an August 2011 monthly composite of MERIS imagery, the lakes within this study could be seperated into two distinct optical water types when their spectral profiles were grouped using a fuzzy clustering approach (Fig. S1). These clusters of spectra closely resemble optical water types six and seven outlined by Moore et al., (2014), which are characterized by a reflectance peak at 560 nm and a secondary peak at 709 nm that is likely the result of strong particle backscattering associated with high algal concentrations.

Of the 1,343 state reported events, 218 were omitted because the corresponding $CI_{cyano}$ observations contained QA flags. The remaining 1,125 state reported events were placed into one of four general observation categories (Fig. 6): cyanotoxins (651), cyanobacteria (379), a combination of cyanobacteria and cyanotoxins (93), or an illness (2). There was a co-occurring $CI_{cyano}$ bloom presence during 69% of state reported events within the cyanotoxin observation category, which was similar to a previously reported study, where overall agreement between $CI_{cyano}$ and state measured cyanotoxin samples was expected to range from 77% to 87% (Mishra et al., 2021). The poorest agreement (42%) occurred between $CI_{cyano}$ bloom presence and state reported events in the cyanobacteria category. Cyanobacteria can be easily misidentified visually by the public or citizen scientists without proper training and the aid of magnification, so states may receive reports from inexperienced individuals that have poor consistency and agreement (Interstate Technology & Regulatory Council, 2021). Because $CI_{cyano}$ was designed to distinguish between cyanoHABs and other algal biomass spectroscopically on the basis of phycocyanin, it could be that many of these state reported events were actually reports of other harmful algal bloom taxa that occur in freshwater such as haptophytes, euglenophytes, raphidophytes, dinoflagellates, chlorophyte, cryptophyte, and diatom

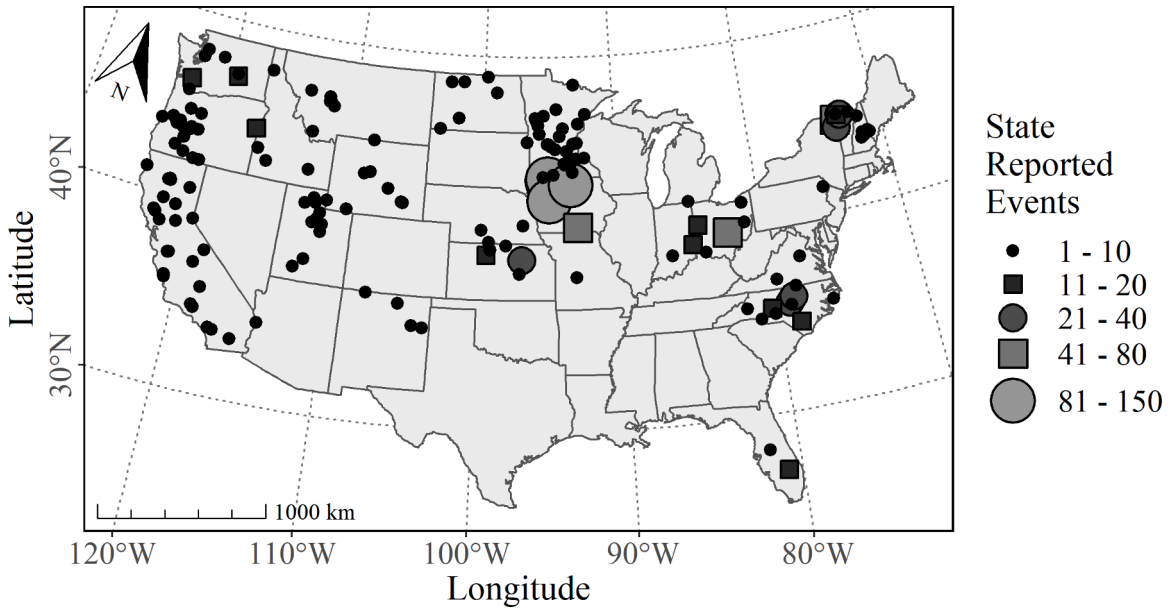


**Fig. 4.** A graduated symbol map of the 1,343 state reported events coincident with $CI_{cyano}$. Each symbol represents a unique lake, and the size of the symbol represents the number of events that occurred in that lake. Circles and rectangles were solely used to help distinguish between the different number of events and have no bearing on any other attribute of the events.

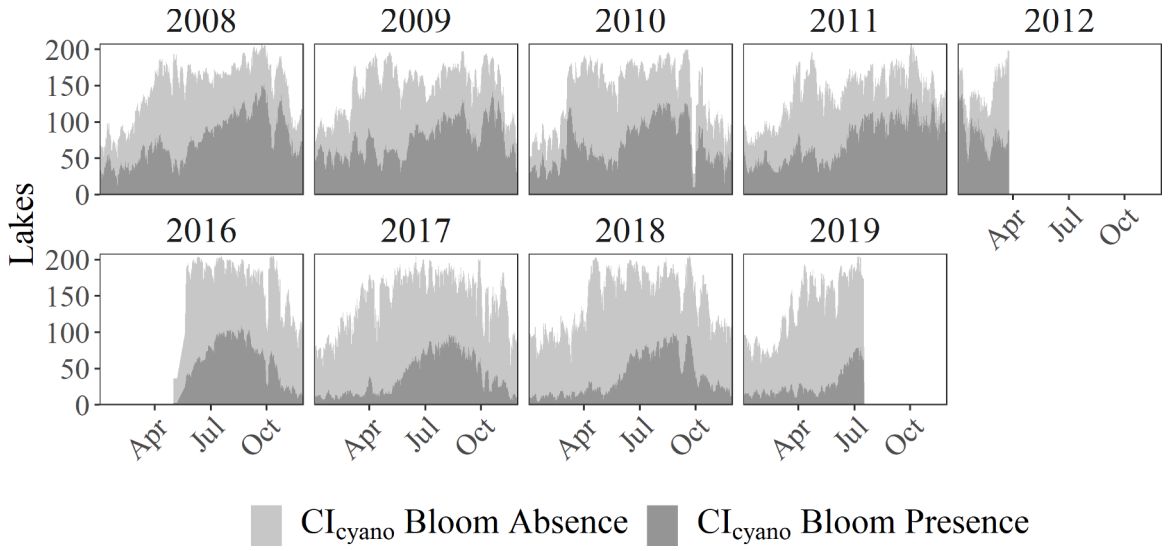


**Fig. 5.** A cumulative time series of $CI_{cyano}$ bloom presence and absence within the 210 unique lakes with state reported events, calculated on a weekly basis during the MERIS and OLCI acquisition periods. The white areas in each panel represent the number of lakes with no satellite retrievals. These $CI_{cyano}$ derived phenological patterns follow previously established ecological patterns of all satellite resolvable lakes across CONUS.

blooms (Papenfus et al., 2020). Mismatches could also be attributed in some cases to nearshore field sampling being spatially removed from where $CI_{cyano}$ measures cyanobacteria offshore. Nearshore accumulations can be driven by wind or wave action with the potential to concentrate cyanobacteria for the entire lake largely on the hydrologically down gradient or downwind shoreline.

In total, out of 1,125 state reported events, 674 (60%) samples were classified as presence-presence and 451 (40%) were classified as misfit absence (Fig. 7). The sensitivity of the true positive rate was demonstrated by modifying the bloom extent and magnitude criteria for $CI_{cyano}$ bloom presence (Table 1). The most sensitive combination of thresholds – a single pixel, anywhere in the lake, with any $CI_{cyano}$ detection greater than or equal to 0.0001 – resulted in the highest true positive rate (77%). However, Coffer et al., (2020) reported that using one-pixel as a threshold might produce more sporadic results than a bloom extent threshold based on a percentage of spatial coverage. Increasing the bloom extent threshold from 10% to 30% of the lake area decreased the true positive rate from 60 to 49%. This was likely due to two factors: (1) more of the lake must have valid and unflagged pixels available for detection and (2) the cyanoHAB biomass must cover a larger portion of the lake, which could lead to the exclusion of smaller, localized events. A more stringent $CI_{cyano}$ bloom magnitude threshold of greater than or equal to 0.001 reduced the true positive rate to ~39% when paired with any of the bloom extent thresholds (Table 1). These results indicate that the lower end of the $CI_{cyano}$ detection limit may be readily observable by humans, which has been previously reported by Coffer et al., (2021b) where qualitative responses from the U.S. EPA's fourth Unregulated Contaminant Monitoring Rule corresponded to $CI_{cyano}$ with an overall

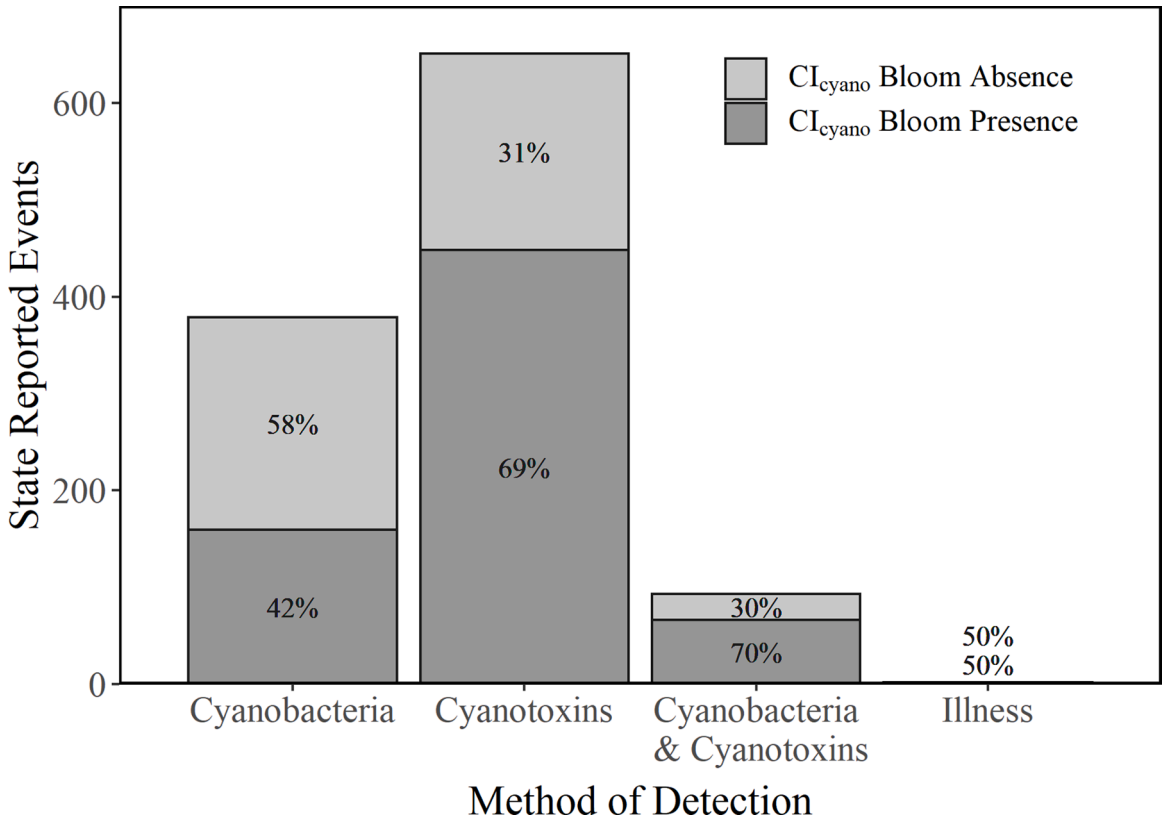


**Fig. 6.** The four general observation categories reported with the records of state reported events along with the percentage of those records with a $CI_{cyano}$ bloom presence or a $CI_{cyano}$ bloom absence. The records of state reported events included in this plot are those that had a coincident satellite observation from MERIS or OLCI with sufficient data for evaluation (n = 1,125).

| $CI_{cyano}$ \ State Reported Events | Presence | Absence | |
|---|---|---|---|
| Presence | 674 (*Presence-Presence*) | - (*Misfit Presence*) | - (*Positive Predictive Value*; eq. 8) |
| Absence | 451 (*Misfit Absence*) | - (*Absence-Absence*) | - (*Negative Predictive Value*; eq. 9) |
| | 60% (*True Positive Rate*; eq. 6) | - (*True Negative Rate*; eq. 7) | - (*Overall Agreement*; eq. 5) |

**Fig. 7.** A confusion matrix with measures of agreement between state reported events and $CI_{cyano}$ bloom presence and absence. A comparison of absence measures was not possible because the state reported event records only contained observations of cyanoHAB presence. There was no documentation for observations of state reported event absence. There were 218 matched state reported events with insufficient satellite data due to quality flagging that were discarded. The true positive rate of $CI_{cyano}$ when compared to state reported events was 60%.

agreement of 94.05% and a Kappa coefficient of 0.70.

The state reported event misfit absences have several explanations. It could be that some of the events were misidentified as cyanobacteria in the field. This can be particularly challenging for citizen science, despite its documented utility in cyanoHAB monitoring (Mishra et al., 2020), because it is often predicated on visual assessments that can make it

**Table 1**
The true positive rate between $CI_{cyano}$ and state recreation events and recreation advisories given different combinations of bloom spatial extent and bloom magnitude thresholds. A $CI_{cyano}$ value of 0.0001 is the algorithm detection limit. A value of 0.001, an order of magnitude higher, was also investigated. The criteria used in the methods of this study and the corresponding true positive rate are italicized and bolded. The true positive rate was used to demonstrate $CI_{cyano}$ sensitivity because it was the only agreement metric that could be calculated for both the state recreation advisories and state reported events.

| $CI_{cyano}$ Spatial Extent | $CI_{cyano}$ Magnitude | State Reported Events True Positive Rate | State Recreation Advisories True Positive Rate |
|---|---|---|---|
| 1 pixel | ≥ 0.0001 | 77% | 80% |
| ***10%*** | ***≥ 0.0001*** | ***60%*** | ***69%*** |
| 20% | ≥ 0.0001 | 53% | 64% |
| 30% | ≥ 0.0001 | 49% | 61% |
| 1 pixel | ≥ 0.001 | 39% | 53% |
| 10% | ≥ 0.001 | 39% | 53% |
| 20% | ≥ 0.001 | 40% | 53% |
| 30% | ≥ 0.001 | 40% | 53% |

difficult to differentiate between cyanoHABs and other algal bloom events that are unrelated to cyanobacteria. In addition to misidentification, some of the reported events may have been present in areas that the satellite could not capture due to their proximity to land, cloud cover, or glint contamination. Finally, it is possible for $CI_{cyano}$ to miss cyanoHAB presences due to algorithmic error or because the cyanobacteria biomass is below the algorithm detection limit due to wind advection or mixing (Mishra et al., 2021).

### 3.2. State recreation advisories

The state recreation advisories that coincided with $CI_{cyano}$ occurred in 87 lakes across 11 states between 2008 and 2019 (Fig. 8). In descending order, the states with the most advisories were California (60), New York (39), Kansas (15), Ohio (11), Wyoming (10), and Oregon (10). The median duration of the state recreation advisories in this study was 42 days (Fig. 9a) and ranged from one day to greater than one year. The three advisories that lasted longer than a year occurred at Grand Lake (commonly referred to as Grand Lake St. Mary's), Ohio; Odell Lake, Oregon; and Lake Berryessa, California. The majority of the advisories started and ended between May and October (Fig. 9b), which overlaps with the typical recreation season that occurs from Memorial Day through Labor Day.

Analyzed by class, a $CI_{cyano}$ bloom presence occurred during 107 of 154 (true positive rate = 69%) recreation advisories, and a reduction in $CI_{cyano}$ or a $CI_{cyano}$ bloom absence occurred after 102 of 134 (true negative rate = 76%) recreation advisories ended (Fig. 10). The positive predictive value was 77% and the negative predictive value was 68% (Fig. 10). Together, this resulted in an overall agreement of 73% and F1 score of 0.73. The F1 score was in the range of previously reported results using *in situ* microcystin toxin detection (0.65) and microcystin observations along with cyanobacteria cell density (0.77) (Mishra et al., 2021). The relatively high F1 score and positive predictive value provide evidence that $CI_{cyano}$ may have utility as a complement to recreation advisory communications (McCarty et al., 2016) for clarifying where and when cyanoHABs occur. These results indicate that $CI_{cyano}$ may be equipped to provide early warnings of cyanoHABs that could assist field efforts to locate cyanobacteria blooms for ground verification and may also be a useful method to ensure a more systematic identification of cyanoHABs in large lakes and reservoirs.

### 3.3. Sensitivity of $CI_{cyano}$ metrics to state recreation advisories

A Wilcoxon signed rank test was used to test the alternative hypothesis that a $CI_{cyano}$ metric derived from data within an advisory period is substantively greater than a $CI_{cyano}$ metric derived from data outside of an advisory period. While each metric was greater during advisory periods than non-advisory times with large positive $z$-scores and low $p$-values, the effect sizes for each metric varied from small to large (Table 2). Specifically, spatial extent had a large effect ($r > 0.5$), magnitude had moderate effect ($r > 0.3$), and temporal frequency had a small effect ($r > 0.1$). The effect size calculated for temporal frequency is likely smaller than magnitude and spatial extent for a few reasons. First, factors like cloud cover, sun glint, and the land-water interface can prevent $CI_{cyano}$ from detecting the presence of a cyanoHABs. Second, the state recreation advisories are not an exhaustive record of every cyanoHAB that occurs within a waterbody, which means that $CI_{cyano}$ may correctly detect a cyanoHAB at times when there are no state recreation advisories. Finally, temporal frequency requires that criteria are used to designate when a $CI_{cyano}$ bloom presence occurs. This is in contrast to magnitude and spatial extent, which are calculated and compared

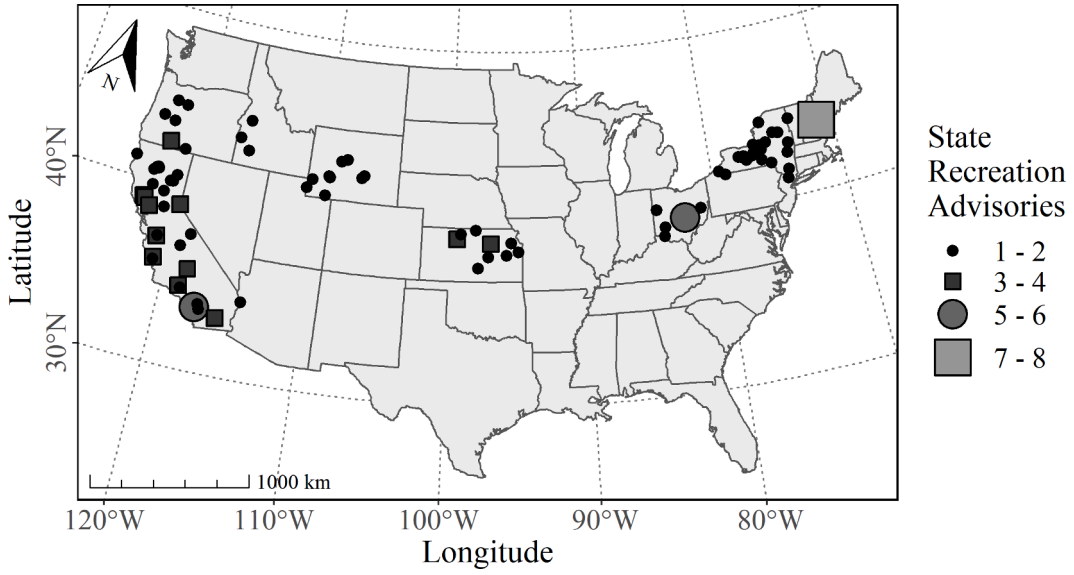


**Fig. 8.** A graduated symbol map of 160 state recreation advisories coincident with $CI_{cyano}$. Each symbol represents a unique lake and the size represents the number of advisories that occurred in that lake. Circles and rectangles were solely used to help distinguish between the different number of events and have no bearing on any other attribute of the events.

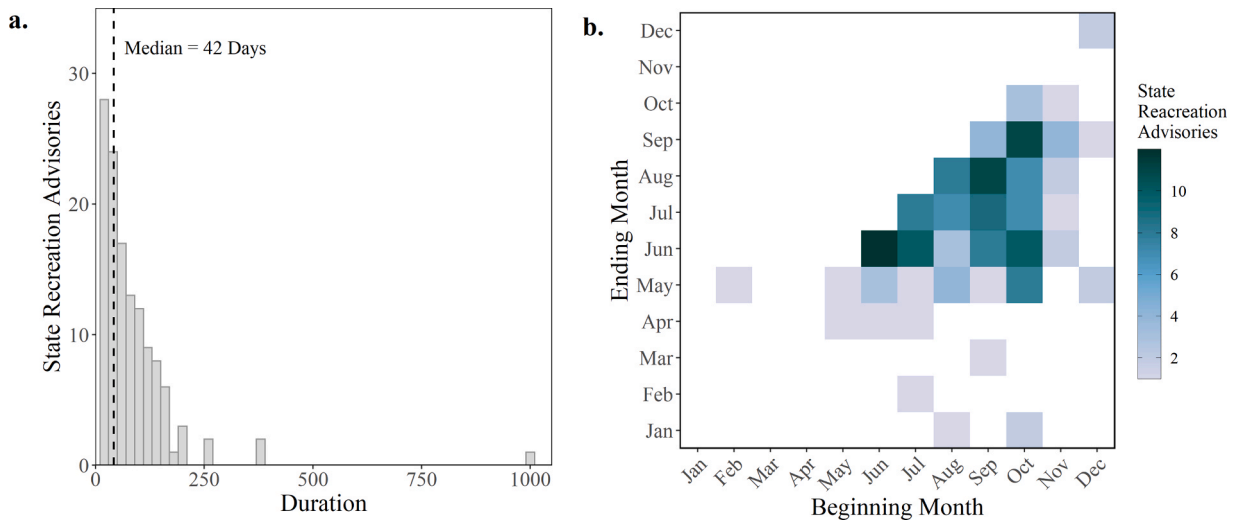


**Fig. 9.** The number of state recreation advisories by duration in days with a bar width of 20 days (a) and the number of state recreation advisories by the month that they started and ended (b).

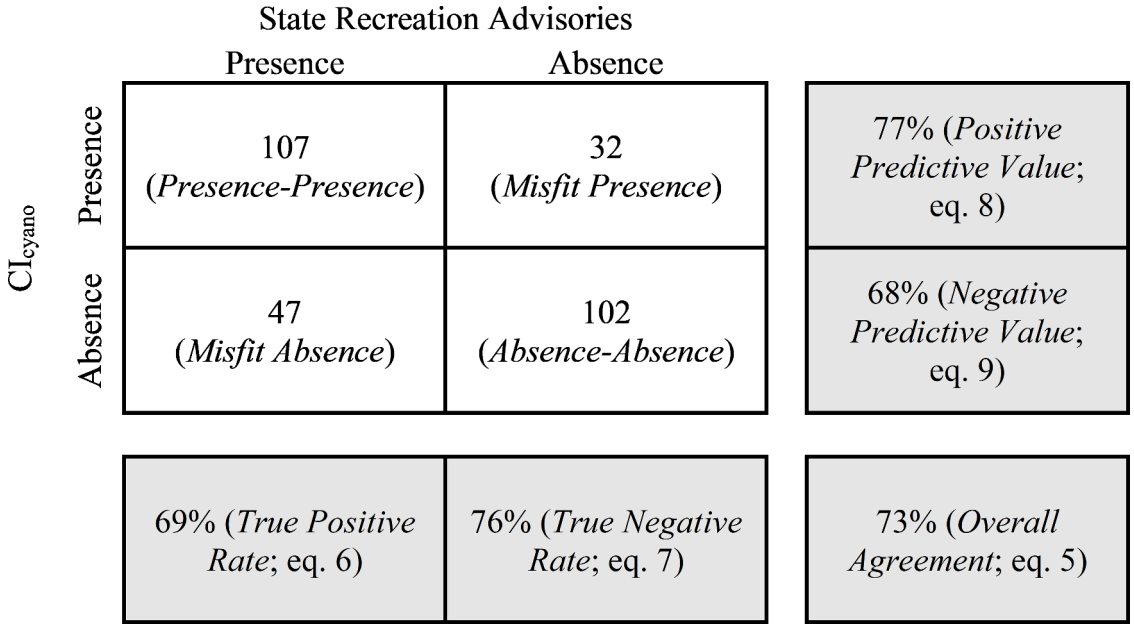


**Fig. 10.** A confusion matrix with measures of agreement between state recreation advisories and $CI_{cyano}$ bloom presence and absence. Although not included in the Fig., the computed F-1 score was 0.73.

without the use of criteria. Together these phenomena may reduce the effect size calculated for temporal frequency, especially when compared to magnitude and spatial extent.

The test was repeated for the recreation season between May 1st and October 31st for all years in the MERIS and OLCI time series to examine the effects of seasonality. As a note, this is also the period when satellite observations are more abundant, $CI_{cyano}$ bloom presence is highest, and state recreation advisories are issued more frequently (Fig. 5; Fig. 9b). The temporal frequency, spatial extent, and magnitude of cyanobacteria derived from $CI_{cyano}$ during the recreation season were each higher during advisory periods compared to non-advisory times (Table 2). In fact, the effect size for each metric during the recreation season followed the same trend as the one displayed when the full OLCI and MERIS acquisition period was examined. $CI_{cyano}$ spatial extent had a large effect ($r > 0.5$), magnitude had moderate effect ($r > 0.3$), and temporal frequency had a small effect ($r > 0.1$). $CI_{cyano}$ summary metrics that are substantively greater during advisories compared to non-advisory times supports the conclusion that the algorithm does have the ability to correctly detect changes in local conditions relevant to recreation advisories, and water quality managers may benefit from using the $CI_{cyano}$ algorithm as an ecological early warning indicator in the future (Butitta et al., 2017; Kefi et al., 2014).

### 3.4. Limitations of the study

There were several limitations of this study given that the state reported event and state recreation advisory data were not collected explicitly for satellite validation, and vice versa. Cyanobacteria follow diel cycling, which results in metabolic alterations that lead to buoyancy regulation (Abeynayaka et al., 2017; Bormans et al., 1999; Chung et al., 2014; Klemer et al., 1996). Optimal satellite observations coincide with solar noon, which usually occurs sometime between 10 a.m. and 2 p.m. local time. Yet, it is common for field crews to start sampling as early as possible in the morning to avoid the hotter afternoons that typically

**Table 2**
Results of the Wilcoxon signed-rank test comparing $CI_{cyano}$ metrics derived from advisory periods to $CI_{cyano}$ metrics derived from non-advisory periods. ***n*** is the number of paired observations with an absolute difference greater than zero and ***W*** is the Wilcoxon signed-rank test statistic.

| $CI_{cyano}$ Metric | Time Frame | *n* | *W* | *z*-score | *p*-value | *r* | *Magnitude* |
|---|---|---|---|---|---|---|---|
| Spatial Extent | Jan 1st – Dec 31st | 61 | 1712 | 5.51 | <0.001 | 0.71 | Large |
| Temporal Frequency | Jan 1st – Dec 31st | 86 | 2386 | 2.22 | 0.013 | 0.24 | Small |
| Magnitude | Jan 1st – Dec 31st | 86 | 2693 | 3.54 | <0.001 | 0.38 | Moderate |
| Spatial Extent | May 1st – Oct 31st | 57 | 1396 | 4.52 | <0.001 | 0.60 | Large |
| Temporal Frequency | May 1st – Oct 31st | 85 | 2442 | 2.69 | 0.004 | 0.29 | Small |
| Magnitude | May 1st – Oct 31st | 85 | 2583 | 3.31 | <0.001 | 0.36 | Moderate |

occur in the summer months. Cyanobacteria are likely to still be migrating vertically towards the photic zone in the morning, which may result in unrepresentative reports of cyanobacteria exposure risk. In addition, while many state reported events and state recreation advisories had coordinate information, those coordinates might represent any combination of lake locations, sampling locations, advisory locations, or any other geographic reference. This meant that coordinates were not used for anything more than identifying the lake location within the state making it impossible to know if a state reported event or state recreation advisory took place in a specific portion of a lake that was not resolvable by satellite data due to cloud cover, sun glint, or the land-water interface.

The land-water interface is a particularly prevelant limitation in this study because many cyanoHAB state reported events and state recreation advisories were most likely predicated on samples or observations made at the shoreline of a lake where people recreate (Backer et al., 2015; Chorus et al., 2000). This also happens to be where cyanobacteria accumulates due to wind advection (Chorus et al., 2000) and where cyanotoxin concentrations tend to be higher (Rogalus and Watzin, 2008). However, the spatial resolution of MERIS and OLCI can prevent measures along these shorelines, which can lead to discrepancies when comparing $CI_{cyano}$ to state reported events and state recreation advisories. An example of the land-water interface problem is provided with Falls Lake, North Carolina, where the recreation beaches have gaps in satellite detection pixels along the shoreline (Fig. 11), and where narrow reaches of the lake may not be resolved. While this study was limited to larger lake systems resolvable by MERIS and OLCI, many lake coves, arms, or slack water areas are prone to scum formation (Stone and Bress, 2007). The spatial resolution limitations of MERIS and OLCI also meant that ~80% of the state records had to be discarded from this study because they occurred in lakes and waterbodies that were not of sufficient size or shape to accommodate at least three, 300-m pixels. In the future, higher resolution satellite missions such as the Landsat series (30 m resolution) and Sentinel-2 (10-60 m resolution) may provide monitoring enhancements in these environments that could lead to greater coincidence with field data, albeit with lower temporal resolution and

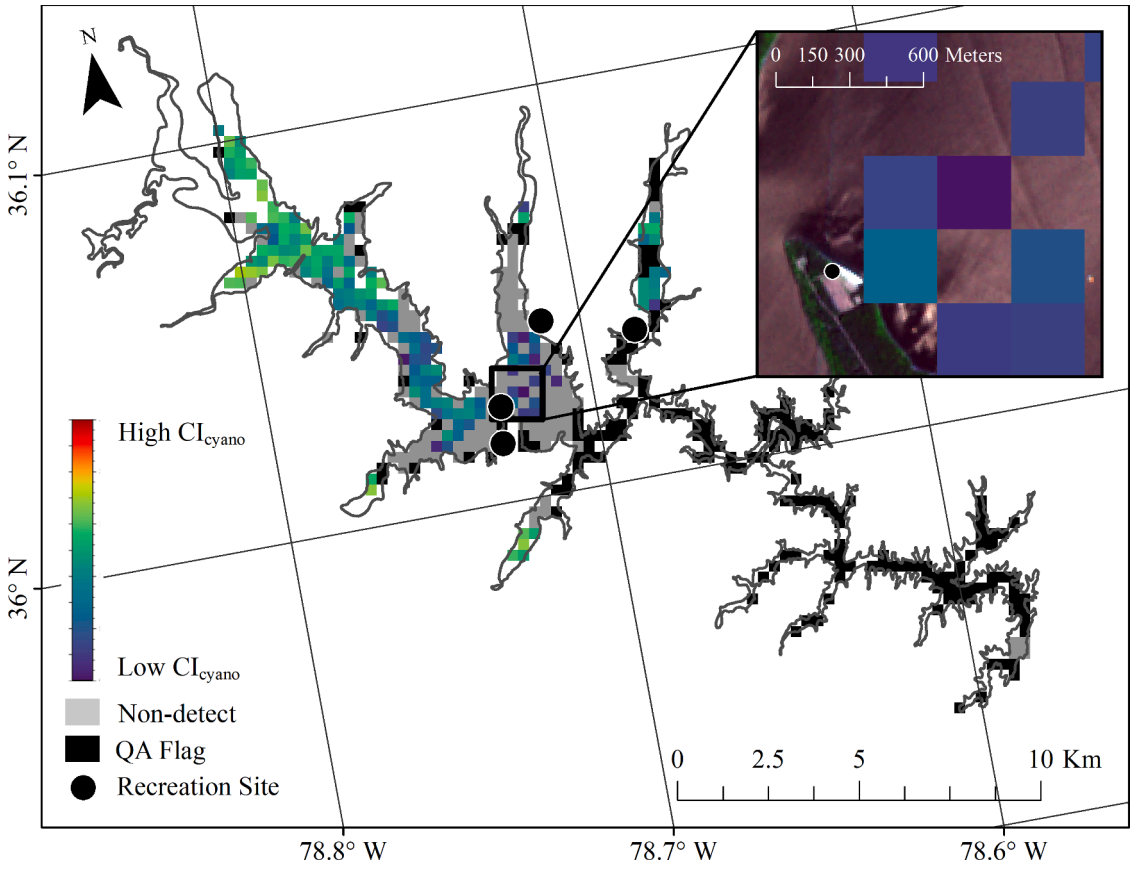


**Fig. 11.** A demonstration of the potential spatial incongruency between recreation sites and satellite pixels using Falls Lake, North Carolina as an example. The colored pixels represent $CI_{cyano}$ estimates of cyanobacteria from low (purple) to high (red). Grey pixels are a valid observation of the lake surface with no detection of cyanobacteria and black pixels were flagged by QA masks. The easternmost recreation site was not close to any satellite water pixels due to the narrow width of the system. While cyanobacteria were detected near one of southern recreation sites, the pixels are still at a distance from shore and may not capture the areas that can be easily sampled in the field. This is highlighted in the inset using a true color image from Sentinel-2 as reference.

reduced ability to differentiate cyanobacteria from other algal biomass.

## 4. Conclusion

Comprehensively monitoring cyanoHABs in the field is challenging due to time, labor, and cost (Papenfus et al., 2020). There is a diverse array of *in situ* methods used for monitoring and detecting cyanoHABs, in addition to a range of thresholds for responding to and issuing advisories (Graham et al., 2009; ITRC 2021), all of which further complicate effective and consistent monitoring and reporting. The behavior of cyanobacteria enhances challenges for monitoring and detection due to temporal and spatial variability and heterogeneity in growth and accumulation, where even weekly scheduled sampling can miss events (Stone and Bress, 2007). Satellite-based monitoring and methods may serve as a complement to traditional *in situ* methods by providing frequent synoptic observations of cyanoHABs that are standardized across space and time.

The primary objective of this study was to validate a satellite-based approach for cyanoHAB monitoring with state reported events and recreation advisories. This is the first study to quantitatively evaluate satellite algorithm performance for detecting cyanoHABs with events and recreation advisories. The combined state reported events and state recreation advisories represented a broad geographical distribution across CONUS commensurate with previously reported human and animal cyanobacterial exposure (Svirčev et al., 2019). This study found that $CI_{cyano}$ detected cyanobacteria presence during 60% of the state reported events and 69% of the state recreation advisories. $CI_{cyano}$ also detected a reduction or absence in cyanobacteria biomass after 76% of the advisories were lifted. The algorithm had an overall agreement of 73% with state advisories, and, while the effect sizes varied from small to large, temporal frequency, spatial extent, and magnitude computed from $CI_{cyano}$ were each greater during state recreation advisories compared to non-advisory times. Therefore, $CI_{cyano}$ does detect a change in cyanobacteria presence during state events and recreation advisories, and it detects a reduction or absence after the advisories end. It also provides differences in cyanoHAB temporal frequency, spatial extent, and magnitude during advisories compared to non-advisory times within the study limitations. The Interstate Technology & Regulatory Council and World Health Organization cyanoHAB monitoring guidelines now recommend remote sensing as a tool to expand the number of water bodies that can be evaluated to improve the development of early warning systems (Chorus and Welker, 2021; Interstate Technology & Regulatory Council, 2021). The work presented in this study directly supports U.S. state managers and their decisions involving satellite technologies that can complement traditional field-based efforts to monitor cyanoHABs.

## Declaration of Competing Interest

The authors declare that they have no known competing financial interests or personal relationships that could have appeared to influence the work reported in this paper.

## Acknowledgments

This work was supported by the National Aeronautics and Space Administration Ocean Biology and Biogeochemistry Program/Applied Sciences Program (proposals 14-SMDUNSOL14-0001 and 20-SMDSS20-0006) and by U.S. Environmental Protection Agency, National Oceanic and Atmospheric Administration, U.S. Geological Survey Toxic Substances Hydrology Program, and Oak Ridge Institute for Science and Education (ORISE). This article has been reviewed by the Center for Environmental Measurement and Modeling and approved for publication. Mention of trade names or commercial products does not constitute endorsement or recommendation for use by the U.S. Government. The views expressed in this article are those of the authors and do not necessarily reflect the views or policies of the U.S. Environmental Protection Agency but do represent the views of the U.S. Geological Survey. All data and code associated with this manuscript is publicly available at DOI: 10.23719/1522957.

## Supplementary materials

Supplementary material associated with this article can be found, in the online version, at doi:10.1016/j.hal.2022.102191.

## References

Abeynayaka, H.D.L., Asaeda, T., Kaneko, Y., 2017. Buoyancy limitation of filamentous cyanobacteria under prolonged pressure due to the gas vesicles collapse. Environ. Manage. 60 (2), 293–303. https://doi.org/10.1007/s00267-017-0875-7.

Austin, B.J., Olsen, B., Wentz, T., Haggard, B.E., 2018. Algal blooms in Arkansas streams, ponds, and lakes. Arkansas Water Resources Center, pp. 1–6.

Backer, L.C., McNeel, S.V., Barber, T., Kirkpatrick, B., Williams, C., Irvin, M., Zhou, Y., Johnson, T.B., Nierenberg, K., Aubel, M., LePrell, R., Chapman, A., Foss, A., Corum, S., Hill, V.R., Kieszak, S.M., Cheng, Y.-S., 2010. Recreational exposure to microcystins during algal blooms in two California lakes. Toxicon 55, 909–921. https://doi.org/10.1016/j.toxicon.2009.07.006.

Backer, L.C., Landsberg, J.H., Miller, M., Keel, K., Taylor, T.K., 2013. Canine cyanotoxin poisonings in the United States (1920s–2012): review of suspected and confirmed cases from three data sources. Toxins 5, 1597–1628. https://doi.org/10.3390/toxins5091597.

Backer, L.C., Manassaram-Baptiste, D., LePrell, R., Bolton, B., 2015. Cyanobacteria and algae blooms: review of health and environmental data from the Harmful Algal Bloom Related Illness Surveillance System (HABISS) 2007–2011. Toxins 7, 1048–1064. https://doi.org/10.3390/toxins7041048.

Binding, C.E., Greenberg, T.A., Bukata, R.P., 2012. An analysis of MODIS-derived algal and mineral turbidity in Lake Erie. J. Great Lakes Res. 38 (1), 107–116. https://doi.org/10.1016/j.jglr.2011.12.003.

Bormans, M., Sherman, B.S., Webster, I.T., 1999. Is buoyancy regulation in cyanobacteria an adaptation to exploit separation of light and nutrients? Marine Freshwater Res. https://doi.org/10.1071/mf99105.

Butitta, V.L., Carpenter, S.R., Loken, L.C., Pace, M.L., Stanley, E.H., 2017. Spatial early warning signals in a lake manipulation. Ecosphere 8 (10). https://doi.org/10.1002/ecs2.1941.

Carmichael, W.W., Boyer, G.L., 2016. Health impacts from cyanobacteria harmful algae blooms: Implications for the North American Great Lakes. Harmful Algae 54, 194–212. https://doi.org/10.1016/j.hal.2016.02.002.

Chorus, I., Falconer, I.R., Salas, H.J., Bartram, J., 2000. Healh risks caused by freshwater cyanobacteria in recreational waters. J. Toxicol. Environ. Health, Part B 3 (4), 323–347. https://doi.org/10.1080/109374000436364.

Chorus, I., Welker, M., 2021. Toxic Cyanobacteria In Water: A Guide To Their Public Health Consequences, Monitoring And Management, 2nd ed. CRC Press. https://doi.org/10.1201/9781003081449.

Chung, S.W., Imberger, J., Hipsey, M.R., Lee, H.S., 2014. The influence of physical and physiological processes on the spatial heterogeneity of a Microcystis bloom in a stratified reservoir. Ecol. Modell. 289, 133–149. https://doi.org/10.1016/j.ecolmodel.2014.07.010.

Clark, J.M., Schaeffer, B.A., Darling, J.A., Urquhart, E.A., Johnston, J.M., Ignatius, A., Myer, M.H., Loftin, K.A., Werdell, P.J., Stumpf, R.P., 2017. Satellite monitoring of cyanobacterial harmful algal bloom frequency in recreational waters and drinking water sources. Ecol. Indic. 80, 84–95. https://doi.org/10.1016/j.ecolind.2017.04.046.

Coffer, M.M., Schaeffer, B.A., Darling, J.A., Urquhart, E.A., Salls, W.B., 2020. Quantifying national and regional cyanobacterial occurrence in US lakes using satellite remote sensing. Ecol. Indic. 111 https://doi.org/10.1016/j.ecolind.2019.105976.

Coffer, M.M., Schaeffer, B.A., Salls, W.B., Urquhart, E., Loftin, K.A., Stumpf, R.P., Werdell, P.J., Darling, J.A., 2021a. Satellite remote sensing to assess cyanobacterial bloom frequency across the United States at multiple spatial scales. Ecol. Indic. 128 https://doi.org/10.1016/j.ecolind.2021.107822.

Coffer, M.M., Schaeffer, B.A., Foreman, K., Porteous, A., Loftin, K.A., Stumpf, R.P., Werdell, P.J., Urquhart, E., Albert, R.J., Darling, J.A., 2021b. Assessing cyanobacterial frequency and abundance at surface waters near drinking water intakes across the United States. Water Res. https://doi.org/10.1016/j.watres.2021.117377.

Cohen, J., 1988. Statistical Power Analysis for the Behavioral Sciences, 2 ed. Lawrence Erlbaum Associates. https://doi.org/10.4324/9780203771587.

Deglint, J.L., Jin, C., Chao, A., Wong, A., 2018. The feasibility of automated identification of six algae types using feed-forward neural networks and fluorescence-based spectral-morphological features. IEEE Access 7, 7041–7053. https://doi.org/10.1109/ACCESS.2018.2889017.

Dodds, W.K., Bouska, W.W., Eitzmann, J.L., Pilger, T.J., Pitts, K.L., Riley, A.J., Schloesser, J.T., Thornbrugh, D.J., 2009. Eutrophication of U.S. freshwaters: analysis of potential economic damages. Environ. Sci. Technol. 43 (1), 12–19. https://doi.org/10.1021/es801217q.

Fritz, C.O., Morris, P.E., Richler, J.J., 2012. Effect size estimates: current use, calculations, and interpretation. J. Exp. Psychol. Gen. 141 (1), 2–18. https://doi.org/10.1037/a0024338.
Graham, J.L., Loftin, K.A., Kamman, N., 2009. Monitoring Recreational Freshwaters. North American Lake Management Society, LakeLine, pp. 18–24.
Graham, J.L., Foster, G.M., Kramer, A.R., 2017. Twenty years of water-quality studies in the Cheney Reservoir Watershed, Kansas, 1996-2016. U.S. Geological Survey. https://doi.org/10.3133/fs20173019.
Hu, C., Lee, Z., Ma, R., Yu, K., Li, D., Shang, S., 2010. Moderate Resolution Imaging Spectroradiometer (MODIS) observations of cyanobacteria blooms in Taihu Lake, China. J. Geophys. Res. 115 (C4) https://doi.org/10.1029/2009jc005511.
Ibelings, B.W., Backer, L.C., Kardinaal, W.E., Chorus, I., 2015. Current approaches to cyanotoxin risk assessment and risk management around the globe. Harmful Algae 49, 63–74. https://doi.org/10.1016/j.hal.2014.10.002.
Ibelings, B.W., Kurmayer, R., Azevedo, S.M.F.d.O.e., Wood, S.A., Chorus, I., Welker, M., 2021. Understanding the occurrence of cyanobacteria and cyanotoxins. Chorus, I., Welker, M. Toxic cyanobacteria in water: A guide to their public health consequences, monitoring and management, 2nd ed. CRC Press. https://doi.org/10.1201/9781003081449.
Interstate Technology & Regulatory Council, 2021. Strategies for preventing and managing harmful cyanobacterial blooms (HCBs). https://hcb-1.itrcweb.org/.
Kefi, S., Guttal, V., Brock, W.A., Carpenter, S.R., Ellison, A.M., Livina, V.N., Seekell, D.A., Scheffer, M., Nes, E.H.v., Dakos, V., 2014. Early warning signals of ecological transitions: methods for spatial patterns. PLoS One 9 (3). https://doi.org/10.1371/journal.pone.0092097.
Klemer, A., Cullen, J., Mageau, M.T., Hanson, K.M., Sundell, R.A., 1996. Cyanobacterial buoyancy regulation: the paradoxical roles of carbon 1. J. Phycol. 32 https://doi.org/10.1111/j.0022-3646.1996.00047.x.
Kutser, T., 2009. Passive optical remote sensing of cyanobacteria and other intense phytoplankton blooms in coastal and inland waters. Int. J. Remote Sens. 30 (4401-4425) https://doi.org/10.1080/01431160802562305.
Luglie, A., Giacobbe, M.G., Riccardi, E., Bruno, M., Pigozzi, S., Mariani, M.A., Satta, C.T., Stacca, D., Bazzoni, A.M., Caddeo, T., Farina, P., Padedda, B.M., Pulina, S., Sechi, N., Milandri, A., 2017. Paralytic shellfish toxins and cyanotoxins in the Mediterranean: new data from Sardinia and Sicily (Italy). Microorganisms 5 (4). https://doi.org/10.3390/microorganisms5040072.
Lunetta, R., Schaeffer, B.A., Keith, D.J., Jacobs, S., Stumpf, R.P., Murphy, M., 2015. Evaluation of cyanobacteria cell count detection derived from MERIS imagery across the eastern USA. Remote Sens. Environ. 157 (24-34) https://doi.org/10.1016/j.rse.2014.06.008.
Lynch, D.R., McGillicuddy, D.J., Werner, F.E., 2009. Skill assessment for coupled biological/physical models of marine systems. J. Mar. Syst. 76, 1–3. https://doi.org/10.1016/j.jmarsys.2008.03.011.
Mann, H.B., Whitney, D.R., 1947. On a test of whether one or two random variables is stochastically larger than the other. Ann. Mathemat. Statis. 18 (1), 50–60. https://doi.org/10.1214/aoms/1177730491.
Matthews, M.W., Bernard, S., Robertson, L., 2012. An algorithm for detecting trophic status (chlorophyll-a), cyanobacterial-dominance, surface scums and floating vegetation in inland and coastal waters. Remote Sens. Environ. 124, 637–652. https://doi.org/10.1016/j.rse.2012.05.032.
Matthews, M.W., Odermatt, D., 2015. Improved algorithm for routine monitoring of cyanobacteria and eutrophication in inland and near-coastal waters. Remote Sens. Environ. 156, 374–382. https://doi.org/10.1016/j.rse.2014.10.010.
McCarty, C.L., Nelson, L., Eitniear, S., Zgodzinski, E., Zabala, A., Billing, L., DiOrio, M., 2016. Community needs assessment after microcystin toxin contamination of a municiple water supply - Lucas County, Ohio, September 2014. Morbid. Mortal. Weekly Report 925–929.
Merel, S., Walker, D., Chicana, R., Snyder, S., Baurès, E., Thomas, O., 2013. State of knowledge and concerns on cyanobacterial blooms and cyanotoxins. Environ. Int. 59, 303–327. https://doi.org/10.1016/j.envint.2013.06.013.
Mishra, D.R., Kumar, A., Ramaswamy, L., Boddula, V.K., Das, M.C., Page, B.P., Weber, S. J., 2020. CyanoTRACKER: A cloud-based integrated multi-platform architecture for global observation of cyanobacterial harmful algal blooms. Harmful Algae 96. https://doi.org/10.1016/j.hal.2020.101828.
Mishra, S., Mishra, D.R., Lee, Z., Tucker, C.S., 2013. Quantifying cyanobacterial phycocyanin concentration in turbid productive waters: A quasi-analytical approach. Remote Sens. Environ. 133, 141–151. https://doi.org/10.1016/j.rse.2013.02.004.
Mishra, S., Stumpf, R.P., Schaeffer, B.A., Werdell, P.J., Loftin, K.A., Meredith, A., 2019. Measurement of cyanobacterial bloom magnitude using satellite remote sensing. Sci. Rep. 9 (1), 1–17. https://doi.org/10.1038/s41598-019-54453-y.
Mishra, S., Stumpf, R.P., Schaeffer, B.A., Werdell, P.J., Loftin, K.A., Meredith, A., 2021. Evaluation of a satellite-based cyanobacteria bloom detection algorithm using field-measured Microcystin data. Sci. Total Environ., 145462 https://doi.org/10.1016/j.scitotenv.2021.145462.
Moore, T.S., Dowell, M.D., Bradt, S., Verdu, A.R., 2014. An optical water type framework for selecting and blending retrievals from bio-optical algorithms in lakes and coastal waters. Remote Sens. Environ. 143, 97–111. https://doi.org/10.1016/j.rse.2013.11.021.
Natural Resource Defence Council, 2019. What's lurking in your lake? An assessment of states' freshwater harmful algal bloom programs. https://www.nrdc.org/harmful-algal-blooms-methodology.
New York Department of Environmental Conservation, 2020. Harmful algal blooms (HAB) program guide.
Ohio Environmental Protection Agency, 2019. Public water system harmful algal bloom response strategy.
Paerl, H.W., 2008. Nutrient and other environmental controls of harmful cyanobacterial blooms along the freshwater–marine continuum. In: Hudnell, H.K. (Ed.), Cyanobacterial Harmful Algal Blooms: State of the Science and Research Needs. Springer, New York, pp. 217–237. https://doi.org/10.1007/978-0-387-75865-7_10.
Paerl, H.W., Hall, N.S., Calandrino, E.S., 2011. Controlling harmful cyanobacterial blooms in a world experiencing anthropogenic and climatic-induced change. Sci. Total Environ. 409 (10), 1739–1745. https://doi.org/10.1016/j.scitotenv.2011.02.001.
Papenfus, M., Schaeffer, B.A., Pollard, A.I., Loftin, K.A., 2020. Exploring the potential value of satellite remote sensing to monitor chlorophyll-a for U.S. lakes and reservoirs. Environ. Monit. Assess. 192 (12), 1–22. https://doi.org/10.1007/s10661-020-08631-5.
Rogalus, M.K., Watzin, M.C., 2008. Evaluation of sampling and screening techniques for tiered monitoring of toxic cyanobacteria in lakes. Harmful Algae 7 (4), 504–514. https://doi.org/10.1016/j.hal.2007.11.002.
Schaeffer, B.A., Loftin, K.A., Stumpf, R.P., Werdell, P.J., 2015. Agencies collaborate, develop a cyanobacteria assessment network. Eos 96 (16-20). https://doi.org/10.1029/2015eo038809.
Schaeffer, B.A., Iiames, J., Dwyer, J., Urquhart, E., Salls, W., Rover, J., Seegers, B., 2018a. An initial validation of Landsat 5 and 7 derived surface water temperature for U.S. lakes, reservoirs, and estuaries. Int. J. Remote Sens. 39 (22), 7789–7805. https://doi.org/10.1080/01431161.2018.1471545.
Schaeffer, B.A., Bailey, S.W., Conmy, R.N., Galvin, M., Ignatius, A.R., Johnston, J.M., Keith, D.J., Lunetta, R.S., Parmar, R., Stumpf, R.P., Urquhart, E.A., Werdell, P.J., Wolfe, K., 2018b. Mobile device application for monitoring cyanobacteria harmful algal blooms using Sentinel-3 satellite Ocean and Land Colour Instruments. Environ. Modell. Softw. 109, 93–103. https://doi.org/10.1016/j.envsoft.2018.08.015.
Shi, K., Zhang, Y., Zhou, Y., Liu, X., Zhu, G., Qin, B., Gao, G., 2017. Long-term MODIS observations of cyanobacterial dynamics in Lake Taihu: Responses to nutrient enrichment and meteorological factors. Sci. Rep. 7, 40326. https://doi.org/10.1038/srep40326.
Siegel, S., 1956. Nonparametric Statistics For The Behavioral Sciences. McGraw-Hill Book Company, Inc.
Simis, S.G.H., Peters, S.W.M., Gons, H.J., 2005. Optical changes associated with cyanobacterial bloom termination by viral lysis. J. Plankton Res. 27 (9), 937–949. https://doi.org/10.1093/plankt/fbi068.
Stone, D., Bress, W., 2007. Addressing public health risks for cyanobacteria in recreational freshwaters: the oregon and vermont framework. Integrat. Environ. Assess. Manag. 3 (1), 137–143. https://doi.org/10.1002/ieam.5630030112.
Stroming, S., Robertson, M., Mabee, B., Kuwayama, Y., Schaeffer, B., 2020. Quantifying the human health benefits of using satellite information to detect cyanobacterial harmful algal blooms and manage recreational advisories in U.S. lakes. GeoHelath. https://doi.org/10.1029/2020GH000254.
Stumpf, R.P., Wynne, T.T., Baker, D.B., Fahnenstiel, G.L., 2012. Interannual variability of cyanobacterial blooms in Lake Erie. PLoS One 7 (8). https://doi.org/10.1371/journal.pone.0042444.
Stumpf, R.P., Davis, T.W., Wynne, T.T., Graham, J.L., Loftin, K.A., Johengen, T.H., Gossiaux, D., Palladino, D., Burtner, A., 2016. Challenges for mapping cyanotoxin patterns from remote sensing of cyanobacteria. Harmful Algae 54, 160–173. https://doi.org/10.1016/j.hal.2016.01.005.
Svirčev, Z., Lalić, D., Savić, G.B., Tokodi, N., Backović•, D.D., Chen, L., Meriluoto, J., Codd, G.A., 2019. Global geographic and historical overview of cyanotoxin distribution and cyanobacterial poisonings. Arch. Toxicol. 93, 2429–2481. https://doi.org/10.1007/s00204-019-02524-4.
U.S. Environmental Protection Agency, 2019a. Cyanobacteria and Cyanotoxins: Information For Drinking Water Systems. U.S. Environmental Protection Agency, Washington, DC.
U.S. Environmental Protection Agency, 2019b. Recommendations for Cyanobacteria And Cyanotoxin Monitoring In Recreational Waters. EPA, Washington, DC, p. 16.
Urquhart, E.A., Schaeffer, B.A., Stumpf, R.P., Loftin, K.A., Werdell, P.J., 2017. A method for monitoring cyanobacterial harmful algal bloom spatial extent using satellite remote sensing data. Harmful Algae 67, 144–152. https://doi.org/10.1016/j.hal.2017.06.001.
Wendt, H.W., 1972. Dealing with a common problem in Social science: A simplified rank-biserial coefficient of correlation based on the U statistic. Eur. J. Soc. Psychol. 2 (4), 463–465. https://doi.org/10.1002/ejsp.2420020412.
Wilcoxon, F., 1945. Individual comparisons by ranking methods. Biometrics Bulletin 1, 80–83. https://doi.org/10.2307/3001968.
Wolf, D., Georgic, W., Klaiber, H.A., 2017. Reeling in the damages: Harmful algal blooms' impact on Lake Erie's recreational fishing industry. J. Environ. Manage. 199, 148–157. https://doi.org/10.1016/j.jenvman.2017.05.031.
World Health Organization, 2003. Algae and cyanobacteria in fresh water, Guidlines for safe recreational water environments, pp. 136-158.
Wynne, T.T., Stumpf, R.P., Tomlinson, M.C., Warner, R.A., Tester, P.A., Dyble, J., Fahnenstiel, G.L., 2008. Relating spectral shape to cyanobacterial blooms in the Laurentian Great Lakes. Int. J. Remote Sens. 29 (12), 3665–3672. https://doi.org/10.1080/01431160802007640.
Wynne, T.T., Stumpf, R.P., Tomlinson, M.C., Dyble, J., 2010. Characterizing a cyanobacterial bloom in western Lake Erie using satellite imagery and meteorological data. Limnol. Oceanogr. 55 (5), 2025–2036. https://doi.org/10.4319/lo.2010.55.5.2025.
Wynne, T.T., Stumpf, R.P., 2015. Spatial and temporal patterns in the seasonal distribution of toxic cyanobacteria in western Lake Erie from 2002–2014. Toxins 7 (5), 1649–1663. https://doi.org/10.3390/toxins7051649.

Wynne, T.T., Meredith, A., Briggs, T., Litaker, W., Stumpf, R.P., 2018. Harmful algal bloom forecasting branch ocean color satellite imagery processing guidelines. NOAA Technical Memorandum NOS NCCOS 252, 48. https://doi.org/10.25923/twc0-f025.

Wyoming Department of Environmental Quality, 2018. Wyoming harmful algal bloom action plan: For publicly accessible lakes and reservoirs of Wyoming.

Xu, H., Paerl, H.W., Zhu, G., Qin, B., Hall, N.S., Zhu, M., 2016. Long-term nutrient trends and harmful cyanobacterial bloom potential in hypertrophic Lake Taihu. China. Hydrobiologia 787 (1), 229–242. https://doi.org/10.1007/s10750-016-2967-4.

Yagoub, M.M., Alsereidi, A.A., Mohamed, E.A., Periyasamy, P., Alameri, R., Aldarmaki, S., Alhashmi, Y., 2020. Newspapers as a validation proxy for GIS modeling in Fujairah, United Arab Emirates: identifying flood-prone areas. Natural Hazards 104, 111–141. https://doi.org/10.1007/s11069-020-04161-y.